

# Green Synthesis of Silver Nanoparticles using *Cardiospermum Halicacabum* Leaf Extract and its Effect on Human Colon Carcinoma Cells

Venkatesan Kotteeswaran\*, Shruthi Ponsreeram, Aritra Mukherjee, Anirudh Sadagopan and Naveen Kumar Anbalagan

Department of Biotechnology, SRM Institute of Science and Technology, Kattankulathur, Tamil Nadu, India.

\*Corresponding Author E-mail: venkatek@srmist.edu.in

<https://dx.doi.org/10.13005/bpj/2915>

(Received: 06 November 2023; accepted: 25 April 2024)

Nanobiotechnology is an evolving domain of scientific exploration connected with synthesis and mechanism of nanoparticles in biological systems. Silver nanoparticles have gained utmost popularity because of its characteristics like thermal conductivity, chemical stability, and high catalytic activities. It also has various advantages like being a drug carrier, transmembrane delivery and potential for controlled intracellular drug-delivery. The current study deals with fabrication of nanoparticles which are formed from biologically reduced silver, followed by its characterization. In addition, anticancer activity was investigated using in-vitro cell model. The synthesis was confirmed from the change in color to brown from golden yellow and also from absorbance peak obtained at 430nm in UV-Vis spectrophotometry. The obtained nanoparticle had an average size of about 150.1 nm and its FTIR peaks suggested the presence of flavonoids and polyphenols. XRD analysis exhibited peaks in the  $2\theta$  range of  $227.72^\circ$ ,  $32.29^\circ$ ,  $38.76^\circ$ ,  $43.17^\circ$ ,  $54.47^\circ$ ,  $64.04^\circ$  and  $77.75^\circ$ , confirms its crystallographic nature. Further, anticancer activity of silver nanoparticles was tested through cell proliferation assays, Lactate Dehydrogenase assays, and apoptosis assay using Hoechst/PI staining, wherein there is clear reduction in cell's proliferation, viability, and LDH release, followed by increased dead cells as a result of treatment.

**Keywords:** Anticancer Activity; Apoptosis; *Cardiospermum halicacabum*; Cell based assay; Green synthesis; Silver nanoparticles.

Nanotechnology is a multidisciplinary field of research having applications in electronics, nanomedicine, aeronautics, biomaterials and energy, cosmetics, and food. Metal nanoparticles such as platinum, silver, and gold are broadly applied in diagnostic sensors, antimicrobials, and as agents for delivery of drug and gene<sup>5,38</sup>. There is a dire need for developing eco-friendly nanomaterial synthesis techniques that prevent harmful by-

products associated with present physicochemical procedures. The relevance of green synthesis in today's times is immense and it must be the only way driving major scientific processes linked to nanotechnology in the future. Green synthesis allows for the reduction in generating any waste that is harmful to the environment, and prevents it by reducing the nanoparticles with the help of biodegradable material like plant extracts, etc.

Hazardous by-products that are unfriendly to nature could be reduced with the help of this method, and is therefore a highly useful procedure to adhere to.

Nanoparticles have greater surface to volume ratio as their size decreases. Specific surface area is important for catalytic reactivity and other features including antibacterial activity. The biological efficiency of nanoparticles can improve when their specific surface area increases due to the rise in surface energy. Many bacterial strains and pathogens typically found in industrial and medicinal operations have been known to be inhibited by silver for a long time. Most of the therapeutic applications commonly utilize silver and silver nanoparticles (AgNPs) due to their medicinal properties. AgNPs of bigger size (100 nm) generate these consequences more efficiently than those of smaller size, although AgNPs of smaller size (10 nm) cause cellular toxicity at a higher degree because they easily enter cells and get localised inside nuclei. AgNPs have unique features, such as conductivity, catalytic properties, nonlinear optical behaviour, chemical stability, and antibacterial activity, for which they have been extensively researched<sup>2</sup>.

Metal nanoparticles can be synthesized and characterized effortlessly and involve easier modification of its surface. Furthermore, it has distinct physiochemical properties like hydrophilicity, optoelectronic property and non-toxicity, which make them a highly demanding nanoscale delivery system. They are widely used as therapeutic agents for several life-threatening ailments including cancer, sexually transmitted diseases, neurological diseases, cardiovascular diseases etc. Also, recent studies have shown that plant-mediated AgNPs demonstrate their anticancer activity by decreasing the rate of malignant cell proliferation through cell-cycle arrest<sup>14</sup>.

Silver nanoparticles are fabricated using several techniques, but chemical techniques are the most prevalent way of producing nanoparticles (AgNPs) among all other technologies. However, there is an inability to prevent the usage of harmful substances in the NP synthesis. Though AgNPs are commonly used in human contact regions, there is an increasing need to create environmentally acceptable nanoparticle syntheses that do not employ harmful chemicals.

In the biological method, plant extracts,

microorganisms, and enzymes are recognized as environmentally safer replacement than physical and chemical nanoparticle synthesis. The capacity to manage and manipulate the concentration of nanoparticles inside cell upto the sustained duration can result in prolonged and effective therapeutic effect and diagnostic sensitivity in biological and clinical applications. Therefore, usage of expensive drugs for cancer therapy would be eliminated because of this unique characteristic of AgNPs. The green synthesis of AgNPs from extracts of various types of plants having unique phytochemical composition contributes to rapid production, enhanced stability, and is very much cost-effective<sup>11</sup>. Treatment using green synthesised AgNPs is sustainable as the nanoparticles are not affected by any physiological factors like enzymes, etc. from within and thus it results in increased bioavailability of therapeutic agent.

The use of medicinal plants has expanded the prospects and treatment options for cancer. They aid in the development of cutting-edge cancer treatment strategies like the green production of AgNPs and serve as a source of new chemicals through phytochemical screening. The *Cardiospermum halicacabum* belonging to Sapindaceae family is a widely known medicinal plant. This plant is cheap and widely available; it is rife with phytochemicals. It contains alkaloids, tannins, flavonoids, glycosides and terpenoids, and is considered highly pertinent in the treatment of cancer. According to reports, *C. halicacabum*'s main chemical components include quercetin 3-O- $\beta$ -D-glucoside, quercetin 3-O- $\alpha$ -L-rhamnoside, quercetin, kaempferol 3-O- $\alpha$ -L-rhamnoside, kaempferol, apigenin 7-O- $\beta$ -D-glucuronidebutylester, apigenin 7-O- $\beta$ -D-glucuronidemethylester, apigenin, and luteolin. These phytochemicals make *Cardiospermum halicacabum* a rich source of antioxidants<sup>(24)</sup>. In cancer treatment, there is an emerging concern towards therapeutic agents using naturally sourced leaves for eco- friendly Ag nanoparticle synthesis. Therefore, it is hypothesized that *Cardiospermum halicacabum* is rich in phytochemicals that may help in inhibition of cancer cells.

Cancer is one of the world's deadliest diseases, killing millions of people every year. Colon cancer ranks third in the world amongst the central reason for cancer related deaths. It emerges

in the colon epithelium which leaps to polyadenoma and from where it finally proliferates to carcinoma stage. Due to various environmental and genetic factors, sedentary lifestyle, alcohol abuse and smoking, there is an increment in Colon cancer. Colon cancer is very badly affecting people across the world and needs proper attention. In this study, AgNPs have been produced, utilizing the extract from the leaf of *Cardiospermum halicacabum*. They have been tested on cell lines for toxicity and anticancer activity.<sup>36</sup>

## MATERIALS AND METHODS

### Preparation of plant extract

*Cardiospermum halicacabum* (Modakathan) leaves were collected from Guduvanchery, Tamil Nadu. The leaves were separated from the collected plant, rinsed with ordinary water and then washed thoroughly several times with Millipore water, to remove debris and other unwanted materials present in it. The leaves were then dried under Sun for few days and kept ready for obtaining the extract. 5g of dried leaves were weighed, followed by finely cutting them into small pieces using sterile scalpel blade. The cut leaves were then added in a sterile beaker containing 100 ml Millipore water. The plant extract was carefully boiled at 60°C for 10 minutes to ensure prevention of phytochemical degradation due to increased temperature. The filtrate of plant extract obtained was then collected by using Whatman filter paper and stored at 4°C until further use.

### Silver nanoparticle synthesis

For synthesis of nanoparticles, the concentration of 1mM of silver nitrate was utilized. 1mL of the extract of leaf was dissolved in 9 mL of silver nitrate and the resultant volume was incubated in dark room for 24 hours at room temperature. It was then spun to observe colour change and then subsequently centrifuged (Thermo Scientific, ST 16R, USA) for 20 min. The supernatant was discarded and pellets of silver nanoparticles were collected and dried in the oven for further analysis.

### UV-Vis spectroscopy analysis

The silver nitrate reduction to AgNP was analysed using UV-Visible Spectrophotometer (Agilent, Cary 60, USA). It is a fast, simple, easy,

and sensitive procedure which analyses the Surface Plasmon Resonance to confirm the presence of silver nanoparticles<sup>(18)</sup>. Strong electromagnetic wave absorption is generally shown by Silver Nanoparticles in the visible range that helps in analysis of Surface Plasmon Resonance. In a quartz cuvette, briefly 2 ml of the reaction mixture was taken and absorption spectrum was recorded in the range from 300 to 800 nm. The spectroscopic readings were taken after 24 hours of incubation.

### Zeta Analyser

Size distribution of bio-reduced AgNPs was measured using Zetasizer (Horiba, SZ-100, Japan). This measures the particle size in dispersed systems from sub-nanometres to several micrometres in diameter. It determines the average size of the particles using photon correlation spectroscopy using Zetasizer which utilises the Brownian motion of the particle to analyse the changes in scattering of light. Furthermore, the net surface charge of the nanoparticles called as Zeta Potential, was also studied to determine the colloidal stability of the nanoparticles<sup>19</sup>. It involves centrifuging the reaction mixture for 20 minutes at 10,000 rpm followed by discarding the supernatant and taking the pellet. Then, the pellets are resuspended in Millipore water and were analysed for Zeta potential. The average size of the particles in terms of the most appropriate one was reported.

### FTIR analysis

FTIR (Shimadzu, Irttracer 100, Japan) analysis was employed for investigating the superior functional groups that are responsible for bio reduction of Ag<sup>+</sup> ions, stabilization, and capping of the AgNPs. This also indicates on how well the functional groups are bonded with each other. The peaks that are obtained in FTIR will provide information on the presence or absence of expected functional groups. Briefly, the synthesized nanoparticles were coated onto KBr, made into thin pellet film and dried before measurements. Potassium bromide is used as a carrier for the sample in IR spectrum because it is transparent in the IR range 500-4000 cm<sup>-1</sup>. Therefore, it doesn't exhibit absorption in this range and no interference would occur in this region. Then, the pellet was subject to FT-IR spectroscopy analysis in the range of 500–4000 cm<sup>-1</sup>.

### XRD analysis

XRD (Bruker, D8 Advance, USA) analyses the nature (crystal or amorphous structure) of silver nanoparticles and the protocol was adapted from <sup>(20)</sup>. The sample was exposed to Energy Dispersion, which involves projecting an X-ray beam onto the sample and disrupting the incident beam scattered by the atoms, resulting in the development of patterns. XRD spectrum checks the quality and formation of compounds. The pattern of XRD was measured using an X-ray diffraction. The powdered sample was obtained as pellet by drying it, which was then loaded onto a glass sample holder and analysed.

### Scanning Electron Microscope analysis (SEM)

SEM (Thermo Scientific, Apreo 2 SEM, USA) was performed to study the morphological nature of silver nanoparticles according to <sup>(30)</sup>. HRSEM uses a high-energy electron beam to scan the silver nanoparticles surface, and then the electrons backscattered were seen to reveal the sample's characteristics. AgNPs were placed on specimen stubs double sided adhesive tape and was subsequently observed under HR-SEM. Finally, the presence of the elements in the nanoparticle was determined by EDX analysis along with SEM.

### Anticancer activity

COLO 205 is a colon cancer cell line, acquired from NCCS, Pune. It was cultured in Roswell Park Memorial Institute Medium (RPMI-1640) using 5% FBS and 1% antibiotic solution incubated in CO<sub>2</sub> incubator at 37 °C.

### Cell proliferation assay

The samples to be studied for cell proliferation were analysed by MTT colorimetric assay using Colo 205 and the methodology was adapted from <sup>(41)</sup>. Here, the MTT assay is used as an investigative tool to analyse the metabolic activity of the cells and to measure their cell proliferation, which could be correlated indirectly with the anti-cancer activity. Briefly, the cultured cells were plated at a density of  $1 \times 10^5$  cells/well in 96-well plate and increasing concentrations of the silver nanoparticles were added to it, followed by incubation for 24 hours. After that, each well plate was treated with 50  $\mu$ L MTT (5mg/mL), followed by 4 hours incubation at 37°C. Finally, the MTT along with the medium were aspirated. Furthermore, 100  $\mu$ L DMSO was affixed as a solvent for Formazan crystals to dissolve, that were

obtained during the experiment. The absorbance was measured using a micro plate reader at 570 nm (Thermo Fisher Scientific, USA).

### Cell viability assay

Trypan blue assay was done to investigate the viability of cells using Colo 205 cells upon administration of drug according to <sup>(41)</sup>. This dye-based test differentiates the dead and live cells depending on the intactness of the cell membranes. The live cells have intact cell membrane whereas it is ruptured in dead cells. Trypan blue is an azo dye which cannot permeate cell membrane, while it can through a ruptured one. Upon seeding of Colo 205 cells, various concentrations of the silver nanoparticles were added to each well for 24 hours. After 24 hours, they were trypsinized, followed by 5 minutes of centrifugation at 1,000 rpm. The pellet obtained was suspended in PBS. Cell suspension was taken and trypan blue was added. Haemocytometer was used to count the number of viable cells. The cells were then viewed under light microscopy. (Leica, Germany).

$$\text{Cell viability (\%)} = (\text{Number of cells which are unstained} / \text{Total number of cells}) \times 100$$

### Cell toxicity assay

The cell toxicity of the sample was measured by the release of Lactate Dehydrogenase (LDH) into the culture media which provides information about the cell membrane disruption. Hence, the LDH Assay was carried out using Colo 205 cells<sup>(22)</sup> by plating the cultured cells on the 96 well plate and treating it with varying concentrations of silver nanoparticles for 24 hours. After 24 hours, the medium was centrifuged at 1500 rpm for 5 minutes and 4 mL of Tris EDTA buffer was mixed with 100 $\mu$ L of supernatant and was incubated for 15 minutes. After incubation, 400  $\mu$ L of sodium pyruvate solution (14 mM) was added to the solution and the absorbance was measured continuously for 3 minutes at 340 nm.

$$\text{LDH activity (\mu M/Min/L)} = (\text{OD change} \times \text{total volume} / \text{min}) / (\text{Sample volume} \times 6.3 \times 10^{-3})$$

### Apoptotic assay

The cell apoptosis study was done by dual fluorescent staining using Hoechst 33342/propidium iodide<sup>(32)</sup>. Briefly, the Colo 205 cells were

plated into 24-well plate and were treated with increasing concentration of silver nanoparticles for 24 hours. After the incubation, the media was aspirated and PBS was used to wash the cells. The wells were stained (50  $\mu$ L HOE, 50  $\mu$ L P1 in 5mL PBS). Following it, the cells underwent 15 minutes incubation in dark at 37°C. The cells were then viewed under fluorescence microscopy (Olympus. CKX-41-TR, Japan).

## RESULTS AND DISCUSSION

Cancer remains a dreaded disease despite technological advancements, capable of tilting the mortality index if not properly attended to<sup>25</sup>. In the year 2020 alone, the newly registered cases of cancer throughout the world, inclusive of all its types, amounts to 10.1 million for men, with about 5.5 million deaths, and 9.2 million for women with about 4.4 million deaths, and most of these deaths had occurred in the Asian countries<sup>10</sup>. Even amongst these cancers, colon cancer is known to be second in mortality relating to cancer, and is known for its trend of occurring mostly in high HDI countries<sup>37</sup>. In order to efficiently treat cancer, newly developed technologies play a major role by effectively overcoming the limitations of conventional treatment. Nanotechnology can play a key role in treating cancer, and its success is evident from the voluminous research papers on that topic published in the current century<sup>15</sup>. It addresses many concerns that conventional therapy fails to address, such as increased solubility of the therapeutic agent, preventing degradation of the drug from various metabolic processes, enhanced specificity of drug action, etc<sup>36</sup>. In this context, Ag nanoparticles were used to encapsulate *Cardiospermum halicacabum* extract in order to efficiently treat cancer.

### Silver nanoparticle synthesis

When the silver nitrate solution was added to the aqueous extract of *Cardiospermum halicacabum* and incubated, the colour of the solution changed to dark brown from yellow as shown in figure 1, which confirmed the synthesis of silver nanoparticles. The colour change occurred as a result of reduction of Ag<sup>+</sup> into Ag<sup>0</sup> by the reducing agent, which are the phytochemicals present in the aqueous extract. These phytochemicals and the related colour

change are the indicators of silver nanoparticle synthesis. The colour shift from golden yellow to dark brown (shown in fig. 1a and 1b) was observed as a result of the reduction reaction mediated by the phytochemicals of plant extract. This is the first observable change that explains the interaction of cationic silver ions with bioactive components of leaf. The obtained change of colour was due to the presence of compounds like alkaloids, phenols, tannins, saponins, triterpenoids, etc., specifically the important carbonyl groups contained therein, that are essential for the bio-reduction of AgNO<sub>3</sub> to Ag nanoparticles,<sup>27,33,34</sup> and also the excitation of the surface plasmon vibrations present in Ag nanoparticles as is confirmed with the UV-vis spectroscopy<sup>26</sup>. The absorption spectra measured in nm for Ag is directly a function of its size and the lesser the diameter of the metal, the more is the scattering of the conducting electrons, which could be one plausible reason for the colour change of nano Ag particles<sup>7</sup>. The oxidation of the hydroxyl groups to carbonyl groups in the solution by Ag ions and themselves getting reduced to elemental Ag is the initial process for the bio-reduction. This process is followed by the oxidation of the hydroxyl groups to potent reducing carbonyl groups like aldehyde by dissolved air, which are responsible for additional reduction of the Ag ions<sup>3</sup>. One useful inference from this is that, the concentration of plant extract in which the Ag ions are dissolved is directly proportional to the bio-reduction of Ag ions. This study is similar with two of the studies that use *Parthenium hysterophorus* leaf extract and *Nocardiopsis dassonvillei* extract wherein similar pattern of colour change was reported suggesting the occurrence of the aforementioned reduction reaction<sup>1,21</sup>

### UV-Vis spectroscopy analysis

The reduction of the silver nitrate to AgNPs was analysed using UV-Visible spectrophotometer. The spectrum has been frequently used to characterize the metal nanoparticles with an absorbance range 300-700 nm. The sample exhibited maximum absorbance value at 430 nm after 24 hours, indicating appropriate silver nitrate reduction to AgNPs as shown in figure 2. Strong electromagnetic wave absorption is generally shown by Silver Nanoparticles in the visible range that indicates the presence of Surface Plasmon Resonance of AgNPs. UV spectral analysis was

performed in order to estimate at what absorbance range do the electrons of Ag absorb maximum light, and that is indicative of whether they have reached nano-size, based on the points mentioned from<sup>29</sup>. UV spectral analysis (shown in fig. 2) showed an absorbance peak at around 430 nm which falls within the range of 400-450 nm; the characteristic range of Ag particles in nano-range<sup>31</sup>. These values are in line with the values obtained from studies that synthesized Ag nanoparticles from soda lime borate glasses, wherein the peaks correspond to 420 nm that comes under the above-mentioned range. They contain similar organic bioactive compounds that mediate the reduction reaction, and the peak

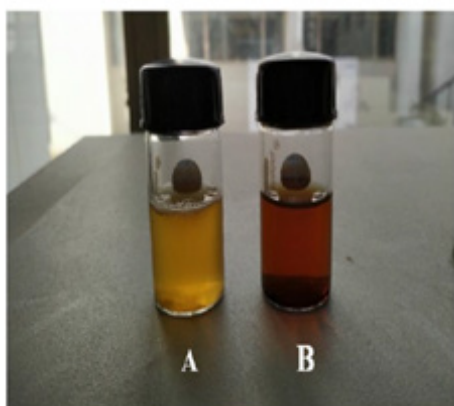


**Fig. 1.** Silver nanoparticles synthesis (A) aqueous leaf extract of *Cardiospermum halicacabum* (B) Silver nanoparticles.

obtained in the same range only corroborates our result<sup>9</sup>.

#### Size and charge analysis

The Zetasizer was used to measure the size of the bio-reduced nanoparticles based upon Brownian motion of the particle upon the illuminated scattered light on the nanoparticle. The principle of Dynamic light scattering is used to scatter light in all directions as the particle is in motion, and thereby measure the intensity of fluctuation of the patches created on a nearby screen as the scattering occurs. The nanoparticle size analysis confirmed that the synthesized AgNPs were extensively dispersed in solution. The mean size of the synthesized nanoparticles was 150.1 nm as shown in figure 3. PI or Polydispersity Index is a measure of how broad the molecular weight distribution is, and falls within the range of 0-1 to indicate if the sample is monodisperse or polydisperse. The PI was also noted to be 0.450 (shown in figure 3). Since the value falls below 0.5, the nanoparticles are found to be monodisperse. Nanoparticles obtained had a zeta average of 150.1 nm (shown in fig. 3) as is concordant with the study that used *Rhus Chinensis* wherein similar size range was reported for the nanoparticles, thereby confirming its applicability on cells<sup>28</sup>. Our PI indicates that the nanoparticles synthesised are of uniform size or are monodisperse, and this uniformity implies that the therapeutic agent, is able to reach the targeted site in optimum amounts,

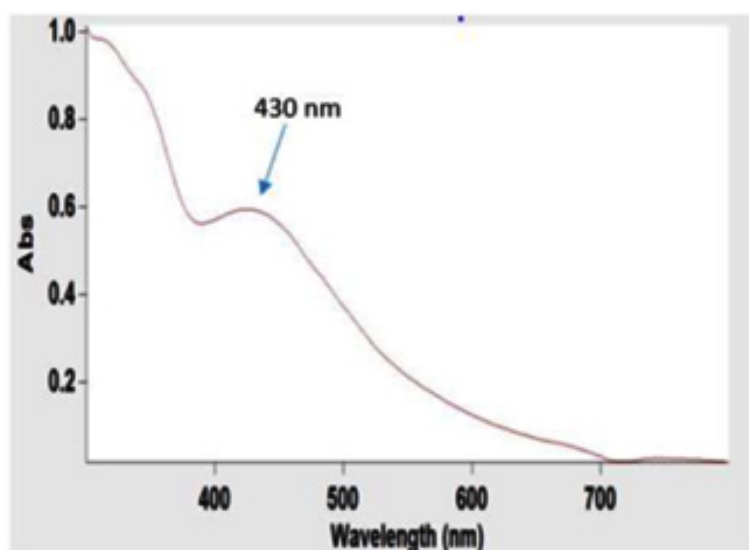


**Fig. 2.** Analysis of silver nanoparticles using UV-Vis spectrum

as nanoparticles that are too big in size (i.e. > 150 nm) would not properly penetrate the cell, and those that are too small would lead to low intracellular bioavailability<sup>23</sup>.

#### FTIR analysis

Fourier Transform Infrared spectroscopy was performed to find the possible functional groups present as shown in figure 4. The peaks obtained in the FTIR report conveys the essential information that the functional groups of the phytochemicals in leaf extract and the nanoparticle have formed a stable nano-complex by showing peaks which

correspond to different functional groups, thereby confirming their presence. Specific band at 3422.04  $\text{cm}^{-1}$  correlates to OH stretching and 2354.16  $\text{cm}^{-1}$  of C-H stretching corresponds to aromatic compounds. However, the peak at 1771.65  $\text{cm}^{-1}$  corresponding to carbonyl group stretching may be representative of phenyl ester. The band at 1274.97  $\text{cm}^{-1}$  is indicative of C-N stretching, corresponding to an aromatic amine, 1580.69  $\text{cm}^{-1}$  indicates N-H bending, representative of primary amines, and 1752.36  $\text{cm}^{-1}$  represents C=O stretching, indicating esters. Peak representing 1063.76  $\text{cm}^{-1}$

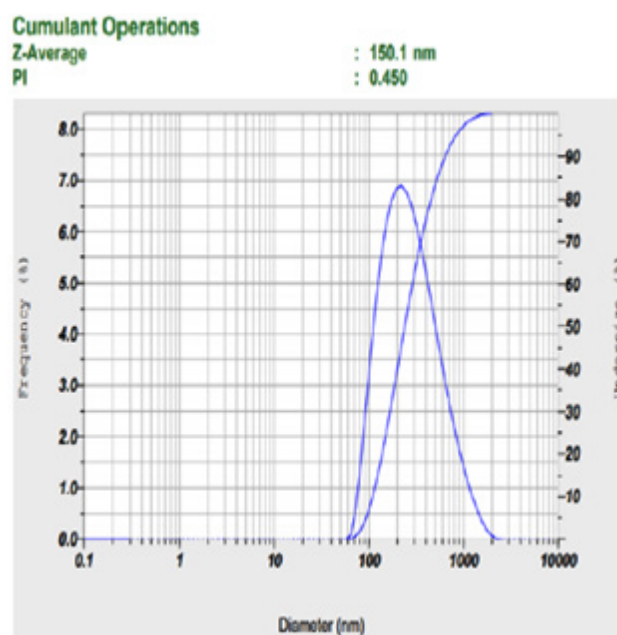


Fig. 3. Zeta analysis of silver nanoparticles.

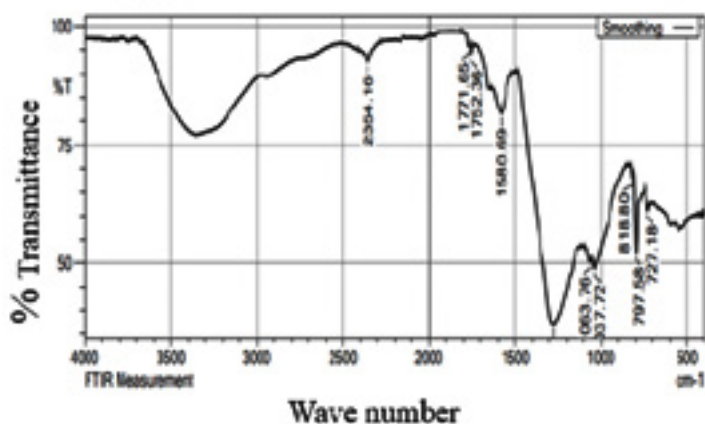


Fig. 4. Characterization of silver nanoparticles using FTIR

is of C-O stretching that corresponds to presence of primary alcohols and  $1037.72\text{ cm}^{-1}$  corresponds S=O stretching, indicative of sulfoxides. These values correspond to functional groups present containing the elements C, H, O, N, and S, which are abundantly present in the organic components

of the plant extract, thereby confirming their role in capping and biological reduction of nanoparticles. Studies relating to the synthesis of Ag nanoparticles show FTIR results wherein peaks corresponding to the same functional groups are observed, especially around  $3477\text{ cm}^{-1}$ ,  $2360.1\text{ cm}^{-1}$ ,  $2342.93\text{ cm}^{-1}$ ,

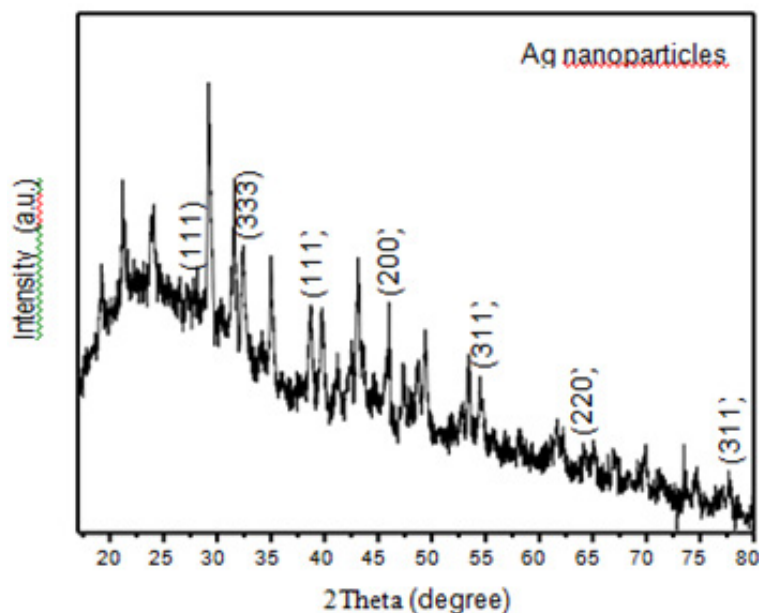


Fig. 5. XRD pattern of the silver nanoparticles

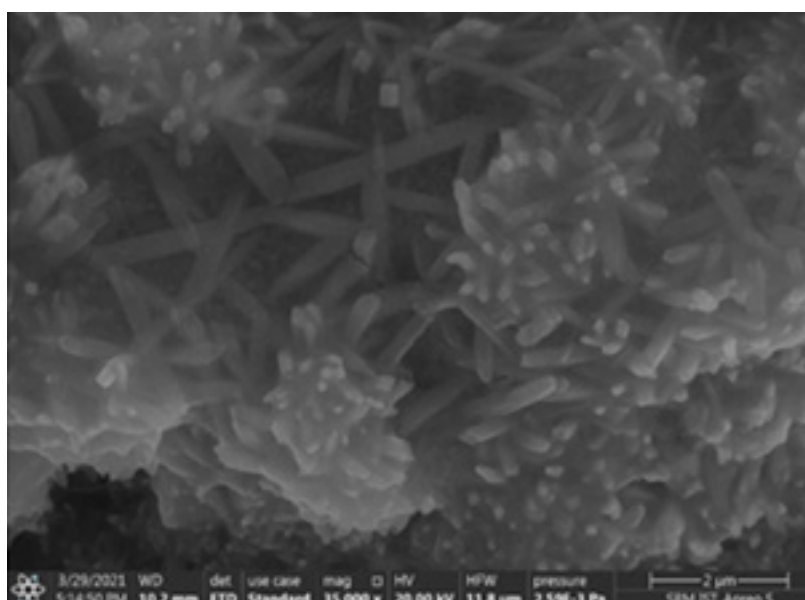


Fig. 6. SEM micrograph of the silver nanoparticles



1762.21  $\text{cm}^{-1}$ , 1657.7  $\text{cm}^{-1}$ , 1398.21  $\text{cm}^{-1}$ , 1038  $\text{cm}^{-1}$ , and 1024  $\text{cm}^{-1}$  thereby corroborating the activity of the functional groups like O-H stretching, C=O stretching, C=C stretching, C-O stretching, C-N stretching, and S=O stretching<sup>31,8</sup>.

#### XRD analysis

XRD analysis is carried out to primarily analyse the structural nature of the nanoparticles formed. The characteristic peaks of silver nanoparticles were further investigated using XRD as shown in the Figure 5. In the pattern of XRD, specific peaks of diffraction were identified

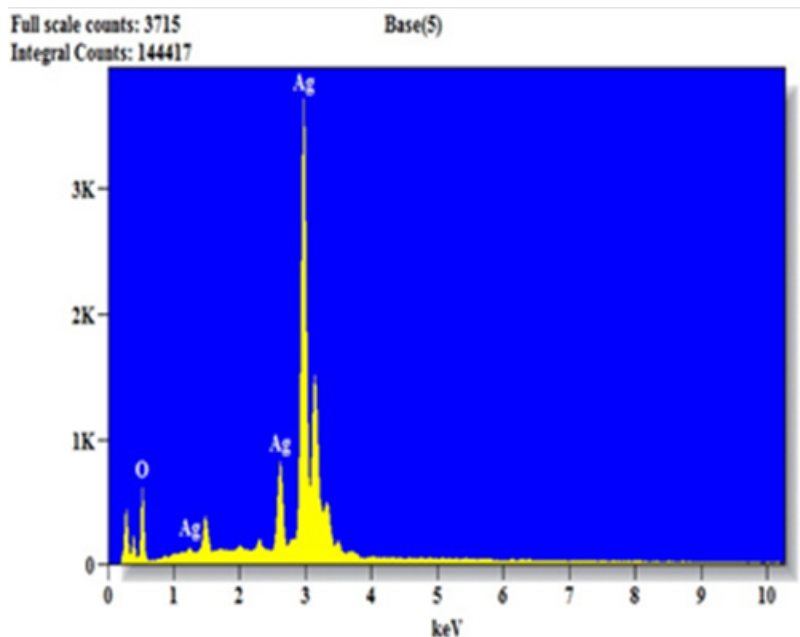


Fig. 7. EDS pattern of synthesized silver nanoparticles

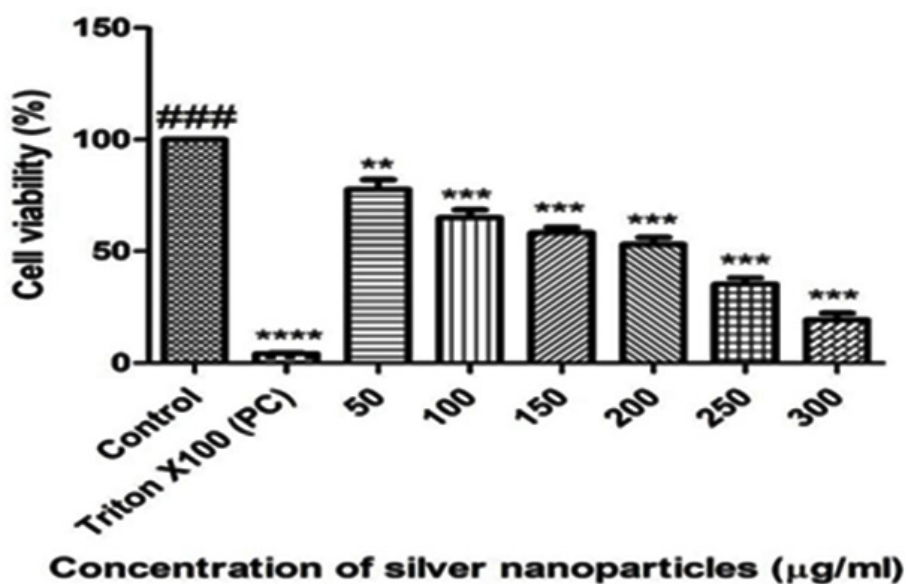


Fig. 8. Cell proliferation of colo 205 after treatment with silver nanoparticles after 24 hours

at 27.72°, 32.29°, 38.76°, 43.17°, 54.47°, 64.04° and 77.75°, all of which correspond to (111), (333), (111), (200), (311), (220) and (111) face-centred cubic (fcc) structure, respectively, which was calculated using Debye–Scherer equation. The results obtained had revealed the crystalline nature of the nanoparticles. The nano-dimensional condition of the synthesized system is inferred from the crisp and wide diffraction pattern such that the many peaks on the particles represent their multi-

faceted growth direction. The broadness in the peak is also thought to be caused by local crystal defects in the nanocrystals. The  $2\theta$  values shown in fig. 5 are in agreement with the reported XRD analysis of 27°, 32°, 46°, 54°, 68° and 77° in silver nanoparticles stabilized by *Eugenia roxburghii*<sup>13</sup>.

#### Scanning Electron Microscopy (SEM)

The SEM analysis is carried out to observe the shape, size and structural studies of the synthesized nanoparticles. Figure 6 has shown

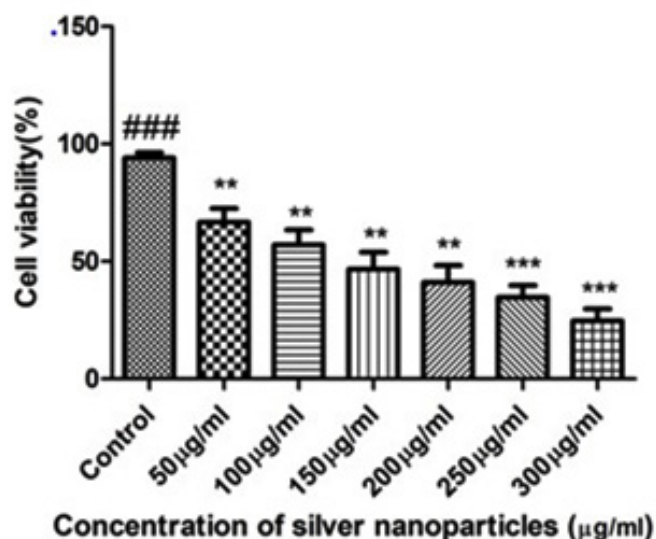


Fig. 9. Viability of Colo 205 after 24 hours of treatment with silver nanoparticles

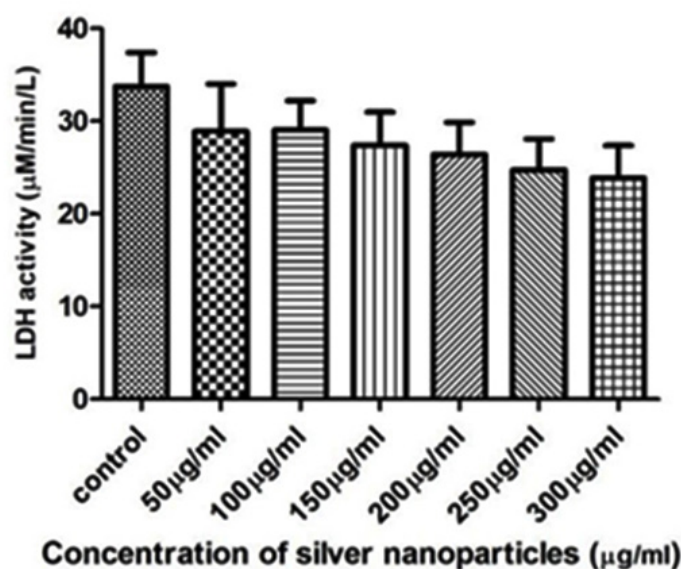


Fig. 10. LDH release after 24 hours of treatment silver nanoparticles at various concentrations

clearly developed Ag nanostructures with large distribution of size, and rod-shaped structures are formed. The silver nanoparticles synthesized showed a large distribution of size. The visible agglomeration of nanoparticles was observed. The bioactive components from aqueous leaf extract of *Cardiospermum halicacabum* were capped with the AgNPs are well exhibited by the visible agglomeration of the nanoparticles in the images obtained. The clustering was found to be similar to studies wherein synthesis of silver nanoparticle was achieved through aqueous leaf extracts of *Alhagi graecorum* in which the obtained silver nanoparticles were clustered and spherical in shape indicating successful stabilisation by phytochemicals<sup>16</sup>. Figure 7 shows the EDS pattern of silver nanoparticles. The peak around 3 KeV confirms the position of elemental silver which is caused as a result of Surface Plasmon resonance in silver nanoparticles. Elemental silver as the major constituent in the nanoparticle was confirmed. The negligible presence of oxygen as evident from the elemental analysis graph might be from the phytochemicals present in the therapeutic agent and is not of any significant consequence to our analysis. The value of obtained peak is in accordance with the analysis of silver nanoparticles using Olive and Green tea extract<sup>4</sup>.

#### Anticancer assays

##### Cell proliferation assay

The cell proliferation assay is performed primarily to check whether there is a decrease in the proliferation of cells when treated with the synthesized nanoparticles, as uncontrolled

proliferation is one undeniable hallmark indicative of cancer. This MTT assay essentially checks for the mitochondrial function, and determines whether the cell is proliferating or not. The in-vitro proliferation effect of AgNPs against colon cancer cell lines (Colo 205) & cell viability (%) was carried out by MTT assay. In this analysis, various concentrations (50-300  $\mu\text{g/mL}$ ) of silver nanoparticles were used to treat the cell-line for 24 hours. We observed that the proliferation rate of colon cancer cells reduced with increase in the amount of silver nanoparticles. From about 75% to 20%, the drop in the rates is evident with the increasing concentration. The cell inhibition which was seen after 24 hours exposure was dose dependent as shown in figure 8. The reduction in the cells percentage with enhancing concentration suggests inhibition of cell proliferation. This inhibition of cell proliferation is indicative of the cell's growth arrest as a response to treatment and thus implies the success of the synthesized nanoparticles. The antiproliferative effect was reported in a similar fashion even for another study wherein AgNPs were synthesized with *Cucumis prophetarum*<sup>17</sup>. Here, a similar dose-dependent decrease in cell proliferation was observed, and upon administering more amounts of synthesized nanoparticles, the cell proliferation decreased. This study utilized various cell lines such as A549, MDA-MB-231, HepG2, and MCF-7, which were checked for its antiproliferative activity, whereby they had different  $\text{IC}_{50}$  values in descending order: 105.8, 81.1, 94.2, and 65.6  $\mu\text{g/mL}$ . Another study that used the aqueous extract of *Acer oblongifolium*, showed anti-proliferative

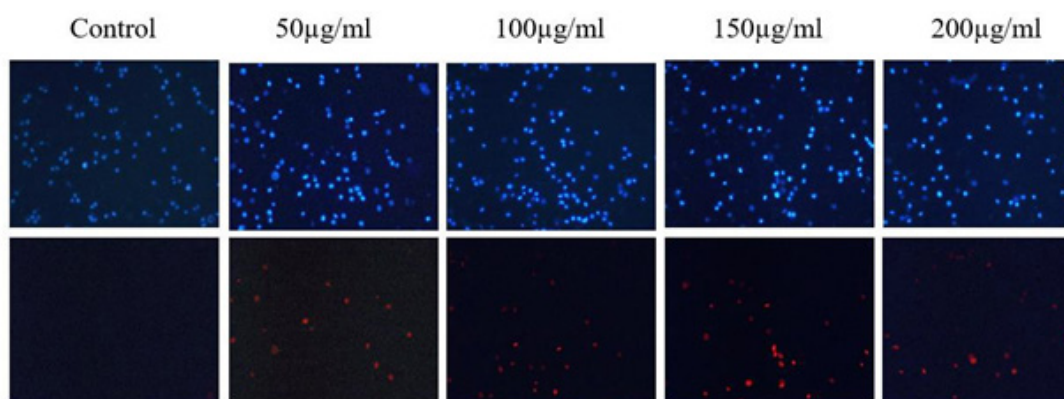


**Fig. 11.** Cell death detection using HOE/PI fluorescent staining after 24 hours of treatment with silver nanoparticles

activity on a comparative basis between MCF-7 and HeLa cells, with the highest activity in MCF-7, and this too was in a dose-dependent manner, i.e. decreased cell proliferation with increased dosage<sup>6</sup>. This proves that our results, being similar to theirs, is thus appropriate.

#### **Cell viability assay**

Cell viability test is performed to evaluate whether the cells are alive or not. After treating the cells with various concentrations (50- 300  $\mu\text{g/mL}$ ) of silver nanoparticles, they were tested for 24 hours to check the number of viable cells, using trypan blue stain. It is quite obvious from the results that the viability of colon cancer cell line decreased with increased concentration from 60 % to about 20%. The drop in cell viability seen after 24 h exposure is shown in the Figure 9. Here, a drop in the cell viability was noted after incubation for 24 hrs post treatment with Ag nanoparticles (fig. 9). The drop was dose-dependent, linear, and gradual, as can be seen from figure 9. Similar decreasing trends in the viability was observed in MCF-7 and A549 cells on treatment with NPs synthesized from *Syzygium aromaticum* extract<sup>35</sup>. Here, the cell viability was tested for treatment with just the plant extract and alongside synthesized Ag nanoparticles, to prove that the latter was much efficient in achieving low cell viability as is similar with our results. In fact, their study even proclaimed that lesser quantity of Ag nanoparticles is required to induce this effect.

#### **Cell toxicity assay**

Cytotoxicity assay through LDH activity evaluation is a good measure of whether post treatment with Ag nanoparticles, there is still cancerous activity. Lactate Dehydrogenase enzyme releases during cell death into the medium. The lactate to pyruvate conversion is catalysed by this enzyme in the presence of  $\text{NAD}^+/\text{NADH}$ . High LDH levels indicate high cytotoxicity and this is a good indicator of cancerous conditions. Thus, estimation of LDH activity confirms whether necrotic cell death or apoptotic cell death has occurred after treatment with silver nanoparticles for 24 h with increasing concentrations (50-300  $\mu\text{g/mL}$ ). The LDH released was quantified after 24 hours of treatment. There is a gradual decrease in the LDH activity from around 27  $\mu\text{M/min/L}$  to about 23  $\mu\text{M/min/L}$  as the concentration increased from 50  $\mu\text{g/ml}$  to 300  $\mu\text{g/ml}$ . There was no significant increase in LDH activity, as shown

in figure 10 which indicated that cell cycle arrest has taken place due to the treatment. The LDH activity showed an increment from 50 to 100  $\mu\text{g/mL}$  wherein the activity increased from 27 to 29  $\mu\text{M/min/L}$ , which was then followed by an overall decreasing trend, from about 29 to 24  $\mu\text{M/min/L}$  and then getting evened in and around the same range (fig. 10). This is indicative of cell growth arrest, which was facilitated by the NPs. This study has results that can be related to another study that uses *Albizia adianthifolia* leaf to synthesize Ag nanoparticles and test it on A549 cell line<sup>12</sup>. Here, the LDH activity is reduced to 36% from 101% following treatment with initially 10  $\mu\text{g/mL}$  and then 50  $\mu\text{g/mL}$  Ag nanoparticles, thereby proving the arrest of cell growth.

#### **Apoptosis assay**

Apoptosis assay was performed to check which of the cells had died as a result of apoptosis, and is measured against treatment with increasing concentration of Ag nanoparticles. The induction of apoptosis was tested using HOE/PI fluorescent staining with treatment of varied concentration of 50-300  $\mu\text{g/mL}$  of silver nanoparticles for 24 hr. Pale blue spots were observed as live cells or early apoptotic cells, as stained by HOE. The distinction could be identified based on the intensity of the colour; higher intensity signifies apoptotic cells as evidenced by the ability of the stain to permeate the cell, while lesser intensity signifies early apoptotic or live cells. The red spots are indication of the stain PI, and they stain late apoptotic cells. The higher the intensity more advanced the apoptotic stage. It can be observed that apoptosis rate of colon cancer cells increased as there is increment in silver nanoparticles concentration. At 150  $\mu\text{g/ml}$ , there are maximum red spots visible as an indication of apoptosis occurring in those many numbers of cells as shown in figure 11. Similarly at 150  $\mu\text{g/ml}$  and 200  $\mu\text{g/ml}$ , the intensity of pale blue spots does increase in a dose-dependent manner, indicating that some cells pass through the early apoptotic phase, an indication of the effect of prepared silver nanoparticles. These results suggest that the AgNPs induce apoptosis on the cells as a reason of morphology change and DNA condensation, indicating that these biologically reduced nanoparticles have apoptotic potential as reported in<sup>39</sup>. In another study, wherein *Clinacanthus nutans* leaves were used to synthesize

Ag nanoparticles and apoptosis was induced, even for low concentrations of Ag nanoparticles such as 4 µg/mL, late apoptosis was induced<sup>40</sup>. The differences in phytochemical composition and amount, also followed by number of nanoparticles formed due to the phytochemicals, could have determined how much of the therapeutic agent acted on the cells to induce the apoptotic pathway.

## CONCLUSION

To summarise the study, the main objective of designing a suitable delivery system for intracellular transportation of the therapeutic agent was successful for the following reasons: the presence of intended functional groups as shown by FTIR data was corroborated by SEM EDX analysis wherein the presence of silver is clearly noted. The intended morphology, size, and charge were achieved through SEM, XRD and Zetasizer, and though negligible deviations existed, it amounts to no big change concerned with the functioning of our system. The XRD values are in line with previous studies and show diffraction peaks indicative of silver, while the Zetasizer highlights the proper size range of the synthesized nanoparticles and also its proper Polydispersity index. Lastly, the most important part that concerns the effect of the drug on cancer cell line Colo 205 was evaluated by several cell-based assays that revealed the efficiency of the drug nanoparticle system on the cancer cell line. A huge drop in the proliferative activity was observed in the cells after the treatment with nanoparticles, followed by a reduction in viability from 60% to 20%, and also minimal LDH activity indicative of anti-cancerous activity, and lastly the increased intensity of the red fluorescence signifies apoptotic activity, all of which cumulatively represents the success of the nanoparticles in eliciting anti-cancer activity. Therefore, in conclusion, a suitable drug delivery system is designed and it shows considerable anti-cancer activity on Colo 205 cell line.

## ACKNOWLEDGMENTS

The authors would like to acknowledge deep regards and gratitude to Dean, School of bioengineering, and HoD, Department of Biotechnology, SRM Institute of Science and

Technology. We also extend our gratitude to the Management of SRM Institute of Science and Technology for providing the facility to complete our project.

## Conflict of Interest

There is no conflict of interest amongst the authors.

## Funding Source

There is no source of financial support.

## REFERENCES

1. Ahsan A, Farooq M. A, Ahsan Bajwa A and Parveen A. Green Synthesis of Silver Nanoparticles Using *Parthenium Hysterophorus*: Optimization, Characterization and In Vitro Therapeutic Evaluation. *Molecules.*, 2020; 25(15): 3324.
2. Alzubaidi A. K, Al-Kaabi W. J, Ali A Al, Albukhaty S, Al-Karagoly H, Sulaiman G. M, Asiri M and Khane Y. Green Synthesis and Characterization of Silver Nanoparticles Using Flaxseed Extract and Evaluation of Their Antibacterial and Antioxidant Activities. *Applied Sciences.*, 2023; 13(4): 2182.
3. Amirjani A and Haghshenas D. F. Ag nanostructures as the surface plasmon resonance (SPR)-based sensors: A mechanistic study with an emphasis on heavy metallic ions detection. *Sens Actuators B Chem.*, 2018; 273: 1768–1779.
4. Bergal A, Matar G. H and Andaç M. Olive and green tea leaf extracts mediated green synthesis of silver nanoparticles (AgNPs): comparison investigation on characterizations and antibacterial activity. *Bionanoscience.*, 2022; 12(2): 307–321.
5. Chandrakala V, Aruna V and Angajala G. Review on metal nanoparticles as nanocarriers: current challenges and perspectives in drug delivery systems. *Emergent Mater.*, 2022; 5(6): 1593–1615.
6. Chinnasamy G, Chandrasekharan S and Bhatnagar S. Biosynthesis of Silver Nanoparticles from *Melia azedarach* Enhancement of Antibacterial, Wound Healing, Antidiabetic and Antioxidant Activities. *Int J Nanomedicine.*, 2019; 14: 9823–9836.
7. Cohen A. C, Roane B. M and Leath C. A. Novel Therapeutics for Recurrent Cervical Cancer: Moving Towards Personalized Therapy. *Drugs.*, 2020; 80(3): 217–227.
8. Dada A. O, Adekola F. A, Dada F. E, Adelani-Akande A. T, Bello M. O, Okonkwo C. R, Inyinbor A. A, Oluyori A. P, Olayanju A, Ajanaku K. O and Adetunji C. O. Silver nanoparticle

- synthesis by *Acalypha wilkesiana* extract: phytochemical screening, characterization, influence of operational parameters, and preliminary antibacterial testing. *Heliyon.*, 2019; 5(10): e02517.
9. El-Kader F. H. A, Hakeem N. A, Osman W. H, Menazea A. A and Abdelghany A. M. Nanosecond Laser Irradiation as New Route for Silver Nanoparticles Precipitation in Glassy Matrix. *Silicon.*, 2019; 11(1): 377–381.
  10. Ferlay J, Colombet M, Soerjomataram I, Parkin D. M, Piñeros M, Znaor A and Bray F. Cancer statistics for the year 2020: An overview. *Int J Cancer.*, 2021; 149(4): 778–789.
  11. Garibo D, Borbón-Núñez H. A, de León J. N. D, García Mendoza E, Estrada I, Toledano-Magaña Y, Tiznado H, Marroquin M. O, Soto-Ramos A. G, Blanco A, Rodríguez J. A, Romo O. A, Chavez-Almazan L. A and Arce A. S. Green synthesis of silver nanoparticles using *Lysiloma acapulcensis* exhibit high-antimicrobial activity. *Sci Rep.*, 2020; 10(1): 12805.
  12. Gengan R. M, Anand K, Phulukdaree A and Chuturgoon A. A549 lung cell line activity of biosynthesized silver nanoparticles using *Albizia adianthifolia* leaf. *Colloids Surf B Biointerfaces.*, 2013; 105: 87–91.
  13. Giri A. K, Jena B, Biswal B, Pradhan A. K, Arakha M, Acharya S and Acharya L. Green synthesis and characterization of silver nanoparticles using *Eugenia roxburghii* DC. extract and activity against biofilm-producing bacteria. *Sci Rep.*, 2022; 12(1): 8383.
  14. Goel M, Sharma A and Sharma B. Recent Advances in Biogenic Silver Nanoparticles for Their Biomedical Applications. *Sustainable Chemistry.*, 2023; 4(1): 61–94.
  15. Haleem A, Javaid M, Singh R. P, Rab S and Suman R. Applications of nanotechnology in medical field: a brief review. *Global Health Journal.*, 2023; 7(2): 70-77.
  16. Hawar S. N, Al-Shmgani H. S, Al-Kubaisi Z. A, Sulaiman G. M, Dewir Y. H and Rikisahedew J. J. Green Synthesis of Silver Nanoparticles from *Alhagigraecorum* Leaf Extract and Evaluation of Their Cytotoxicity and Antifungal Activity. *J Nanomater.*, 2022; 2022: 1–8.
  17. Hemlata, Meena P. R, Singh A. P and Tejavath K. K. Biosynthesis of Silver Nanoparticles Using *Cucumis prophetarum* Aqueous Leaf Extract and Their Antibacterial and Antiproliferative Activity Against Cancer Cell Lines. *ACS Omega.*, 2020; 5(10): 5520–5528.
  18. Isa N, Osman M. S, Abdul Hamid H, Inderan V and Lockman Z. Studies of surface plasmon resonance of silver nanoparticles reduced by aqueous extract of shortleaf spikes edge and their catalytic activity. *Int J Phytoremediation.*, 2023; 25(5): 658–669.
  19. Jakinala P, Lingampally N, Hameeda B, Sayeed R. Z, Khan M. Y, Elsayed E. A and Enshasy H. E. Silver nanoparticles from insect wing extract: Biosynthesis and evaluation for antioxidant and antimicrobial potential. *PLoS One.*, 2021; 16(3): e0241729.
  20. Kanniah P, Radhamani J, Chelliah P, Muthusamy N, Joshua Jebasingh Sathiya Balasingh E, Reeta Thangapandi J, Balakrishnan S and Shanmugham R. Green Synthesis of Multifaceted Silver Nanoparticles Using the Flower Extract of *Aervalanata* and Evaluation of Its Biological and Environmental Applications. *Chemistry Select.*, 2020; 5(7): 2322–2331.
  21. Khalil M. A, El-Shanshoury A. E. R. R, Alghamdi M. A, Alsalmi F. A, Mohamed S. F, Sun J and Ali S. S. Biosynthesis of Silver Nanoparticles by Marine Actinobacterium *Nocardioopsis dassonvillei* and Exploring Their Therapeutic Potentials. *Frontiers in Microbiology.*, 2022; 12: 705673.
  22. Khan Md. R, Hoque S. M, Hossain K. F. B, Siddique Md. A. B, Uddin Md. K and Rahman Md. M. Green synthesis of silver nanoparticles using *Ipomoea aquatica* leaf extract and its cytotoxicity and antibacterial activity assay. *Green Chem Lett Rev.*, 2020; 13(4): 303–315.
  23. Lee Y. J and Park Y. Green Synthetic Nanoarchitectonics of Gold and Silver Nanoparticles Prepared Using Quercetin and Their Cytotoxicity and Catalytic Applications. *J Nanosci Nanotechnol.*, 2020; 20(5): 2781–2790.
  24. Linh N. T. T, Cham B. T, Anh N. T. H, Quan T. D, Nhung L. T. H, Thang L. Q, Adoriso S, Delfino D. V and Thuy T. T. Flavonoid from the aerial parts of *Cardiospermum halicacabum* L. *Vietnam Journal of Chemistry.*, 2023; 61(1): 80–83.
  25. Mattiuzzi C and Lippi G. Current Cancer Epidemiology. *J Epidemiol Glob Health.*, 2019; 9(4): 217.
  26. Morais M, Teixeira A. L, Dias F, Machado V, Medeiros R and Prior J. A. V. Cytotoxic Effect of Silver Nanoparticles Synthesized by Green Methods in Cancer. *J Med Chem.*, 2020; 63(23): 14308–14335.
  27. Osorio-Echavarría J, Osorio-Echavarría J, Ossa-Orozco C. P and Gómez-Vanegas N. A. Synthesis of silver nanoparticles using white-rot fungus *Anamorphous Bjerkandera* sp. R1: influence of silver nitrate concentration and fungus growth time. *Sci Rep.*, 2021; 11(1): 3842.
  28. Patil M. P, Rokade A. A, Ngabire D and Kim G. D. Green Synthesis of Silver Nanoparticles Using

- Water Extract from Galls of *Rhus Chinensis* and Its Antibacterial Activity. *J Clust Sci.*, 2016; 27(5): 1737–1750.
29. Rakib-Uz-Zaman S. M, Hoque Apu E, Muntasir M. N, Mowna S. A, Khanom M. G, Jahan S. S, Akter N, Khan M. A. R, Shuborna N. S, Shams S. M and Khan K. Biosynthesis of Silver Nanoparticles from *Cymbopogon citratus* Leaf Extract and Evaluation of Their Antimicrobial Properties. *Challenges.*, 2022; 13(1): 18.
30. Sarli S, Kalani M. R and Moradi A. A Potent and Safer Anticancer and Antibacterial-Based Green Synthesized Silver Nanoparticle. *Int J Nanomedicine.*, 2020; 15: 3791–3801.
31. Singla S, Jana A, Thakur R, Kumari C, Goyal S and Pradhan J. Green synthesis of silver nanoparticles using *Oxalis griffithii* extract and assessing their antimicrobial activity. *Open Nano.*, 2022; 7: 100047.
32. Sritharan S and Sivalingam N. Curcumin induced apoptosis is mediated through oxidative stress in mutated p53 and wild type p53 colon adenocarcinoma cell lines. *J Biochem Mol Toxicol.*, 2021; 35(1): e22616.
33. Tailor G, Yadav B. L, Chaudhary J, Joshi M and Suvalka C. Green synthesis of silver nanoparticles using *Ocimumcanum* and their anti-bacterial activity. *Biochem Biophys Rep.*, 2020; 24: 100848.
34. Vanlalveni C, Lallianrawna S, Biswas A, Selvaraj M, Changmai B and Rokhum S. L. Green synthesis of silver nanoparticles using plant extracts and their antimicrobial activities: a review of recent literature. *RSC Adv.*, 2021; 11(5): 2804–2837.
35. Venugopal K, Rather H. A, Rajagopal K, Shanthi M. P, Sheriff K, Illiyas M, Rather R. A, Manikandan E, Uvarajan S, Bhaskar M and Maaza M. Synthesis of silver nanoparticles (Ag NPs) for anticancer activities (MCF 7 breast and A549 lung cell lines) of the crude extract of *Syzygium aromaticum*. *J Photochem Photobiol B.*, 2017; 167: 282–289.
36. Wahab S, Alshahrani M. Y, Ahmad M. F and Abbas H. Current trends and future perspectives of nanomedicine for the management of colon cancer. *Eur J Pharmacol.*, 2021; 910: 174464.
37. Wong M. C. S, Huang J, Lok V, Wang J, Fung F, Ding H and Zheng Z. J. Differences in Incidence and Mortality Trends of Colorectal Cancer Worldwide Based on Sex, Age, and Anatomic Location. *Clinical Gastroenterology and Hepatology.*, 2021; 19(5): 955-966.
38. Xu J. J, Zhang W. C, Guo Y. W, Chen X. Y and Zhang Y. N. Metal nanoparticles as a promising technology in targeted cancer treatment. *Drug Deliv.*, 2022; 29(1): 664–678.
39. Xu Z, Feng Q, Wang M, Zhao H, Lin Y and Zhou S. Green Biosynthesized Silver Nanoparticles With Aqueous Extracts of *Ginkgo biloba* Induce Apoptosis via Mitochondrial Pathway in Cervical Cancer Cells. *Front Oncol.*, 2020; 10: 575415.
40. Yakop F, Abd Ghafar S. A, Yong Y. K, Saiful Yazan L, Mohamad Hanafiah R, Lim V and Eshak Z. Silver nanoparticles *Clinacanthus Nutans* leaves extract induced apoptosis towards oral squamous cell carcinoma cell lines. *Artif Cells Nanomed Biotechnol.*, 2018; 46(2): 131–139.
41. Yuan Y. G, Cai H. Q, Wang J. L, Mesalam A, Md Talimur Reza A. M, Li L, Chen L and Qian C. Graphene Oxide–Silver Nanoparticle Nanocomposites Induce Oxidative Stress and Aberrant Methylation in Caprine Fetal Fibroblast Cells. *Cells.*, 2021; 10(3): 682.